

Title:	Mitigation of Current Harmonics in Inverter-Fed Permanent Magnet Synchronous Machines with Nonlinear Magnetics
Authors:	Jan Richter, Thomas Lannert, Tobias Gemassmer, Martin Doppelbauer
Institute:	Karlsruhe Institute of Technology (KIT) Elektrotechnisches Institut (ETI) Hybrid Electric Vehicles (HEV)
Type:	Conference Proceedings
Published at:	Proceedings 2015 PCIM Europe, International Conference and Exhibition for Power Electronics, Intelligent Motion, Renewable Energy and Energy Management, Nuremberg, Germany, May 19-21, 2015 Publisher: VDE Verlag Year: 2015 ISBN: 978-3-8007-3924-0 Pages: 725-732
Hyperlinks:	<a href="#">IEEE Xplore Digital Library</a>

# Mitigation of Current Harmonics in Inverter-Fed Permanent Magnet Synchronous Machines with Nonlinear Magnetics

Jan Richter, Thomas Lannert, Tobias Gemassmer, Martin Doppelbauer  
 Elektrotechnisches Institut (ETI) – Hybrid Electric Vehicles  
 Karlsruhe Institute of Technology (KIT), Kaiserstr. 12, 76131 Karlsruhe, Germany  
 Tel.: +49 721 608 41907, E-Mail: Jan.Richter@kit.edu

## Abstract

Inverter nonlinearities and machine spatial harmonics yield unwanted machine current harmonics, causing control loop instabilities, additional losses and torque ripples. In this paper a method is presented that allows online identification and compensation of both effects for anisotropic permanent magnet synchronous machines with nonlinear magnetics. The method requires no additional sensors and only fundamental component machine model parameters. It can be implemented easily in existing inverter systems by software updates. Test bench measurements show significant improvements in the whole operational area. Measurements at nominal operation result in a motor current total harmonic distortion of 0.28 % which is less than a seventh of the uncompensated value. The functional principle is transferable to other machine types or grid applications enabling the mitigation of current harmonics in a wide field of applications.

## 1. Introduction

The influences of motor current harmonics in inverter-fed drives are well known [1-5]. They are caused by three effects: inverter switching, inverter nonlinearities and spatial harmonics of the machine. All three effects yield voltage harmonics that generate phase currents harmonics. Harmonics due to inverter switching are unavoidable since they follow the used working principle of the DC/AC inverter and the pulse-frequency related modulation scheme. Harmonics created by inverter nonlinearities can be mitigated. Most known approaches use an inverter model for that purpose. Model parameters are either obtained from product data sheets [1, 2], characterization measurements [6] or a combination of the two [3, 5]. Depending on model complexity the inverter dead-time [1, 3, 6], current zero-clamping [2, 5] and diode capacity effects [5] are considered. Some methods partly work online to adapt parameters [5] or to determine the current zero-crossing more precisely [3]. Obviously, all inverter models

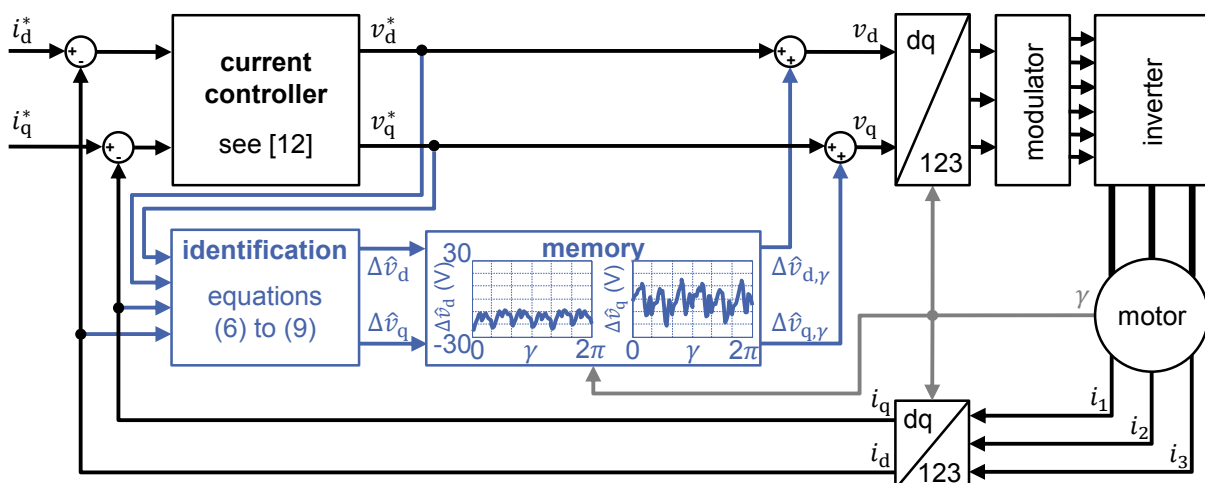


Fig. 1 Scheme of the proposed method. The currents  $i_k$  with  $k \in \{d, q\}$  are closed loop controlled to their reference values  $i_k^*$ . The essentials of the proposed method are marked blue. Voltage errors  $\Delta \hat{v}_k$  are identified online, stored in dependence on the rotor angle  $\gamma$  and feed-forward controlled.

contain errors and taking all physical effects into account results in complex models and extensive parameterization. Hence, a method that estimates and compensates the overall inverter voltage error online was proposed [4]. The inverter voltage error is identified in one control period and feed-forward controlled in the next. However, this will only work if the voltage error does not change from one control period to another.

Other approaches mitigate current harmonics caused by machine spatial harmonics. It was shown that the 6<sup>th</sup> harmonic of the rotor-oriented dq-currents can be mitigated by including filters [7] or by precise characterization measurements and feed-forward control [8]. Both methods use offline parameterization and lookup tables. That is why usage of parameters obtained from one sample for multiple specimens in series production is questionable [8]. The methods only work for machines with equal inductances in the direct and quadrature axes and mitigate only one distinct frequency.

The proposed method mitigates current harmonics caused both by inverter nonlinearities and machine spatial harmonics. As given in Fig. 1 it is integrated in a rotor-oriented current controller and based on two ideas:

- First, the online identification of the total voltage errors  $\Delta\hat{v}_k$  by using the controller reference voltages  $u_k^*$ , the measured currents  $i_k$  and the rotor angle  $\gamma$  with  $k \in \{d, q\}$ .
- Second, the principle of repetitive control because the voltage errors are stored in dependence on the rotor angle that repeats periodically. Feed-forward control of the stored voltage errors  $\Delta\hat{v}_{k,\gamma}$  yields remarkable mitigation. Repetitive control was already applied to remove periodical errors in speed and position control of hard disc [9] and optical disk drives [10].

Mitigation works best during stationary operation because then the total voltage errors are periodical. During transients the compensation of voltage errors is not a prior objective, because a good controller utilizes the maximal inverter output voltage anyway. The method works for any kind of permanent magnet synchronous machine because both nonlinear magnetics and magnetic anisotropy of the rotor are covered. All harmonics are mitigated, which is only restricted by the physical limits of the system given by the sampling frequency or rather the sampling theorem and the voltage limit of the inverter. Implementation on a micro-controller is simple as the number of calculations and the need of additional dynamic memory is very little. The functional principle is transferable to other machine types or grid applications, enabling the mitigation of current harmonics in a wide field of applications.

In the next Section the inverter and the machine model is introduced before the online harmonic mitigation method is developed theoretically. Implementation and the test bench are described in Section three. Measurement results and mitigation performance of the machine under test are discussed in Section four before the most important results are summarized in Section five.

## 2. Theory

### 2.1. Machine and Inverter Model

Permanent magnet synchronous machines have been extensively studied. Validated models that include the nonlinear effects of saturation, cross-coupling and spatial harmonics are described in [7, 8, 11] and briefly summarized here. The machine is assumed to have three symmetric star-connected phases with the neutral point not connected to the inverter. Dielectric currents, iron and friction losses are disregarded. The stator voltages can then be calculated by employing Ohm's law, Faraday's law of induction and Kirchhoff's laws to the machine's coils. Subsequent transformation to the rotor-fixed dq-reference frame yields the system equations.

$$v_d = Ri_d + \frac{d\Psi_d}{dt} - \omega\Psi_q \quad (1)$$

$$v_q = Ri_q + \frac{d\Psi_q}{dt} + \omega\Psi_d \quad (2)$$

Therein  $t$  denotes the time,  $R$  the ohmic resistance,  $\omega$  the electric angular frequency,  $v_k$  the stator voltage,  $i_k$  the stator current and  $\Psi_k$  the stator flux linkage with  $k \in \{d, q\}$ . The flux

linkage  $\Psi_k$  depends nonlinearly on both the currents to account for saturation and cross-coupling and on the rotor angle  $\gamma$  to include spatial harmonics.

$$\Psi_d = f(i_d, i_q, \gamma) \text{ and } \Psi_q = g(i_d, i_q, \gamma) \quad (3)$$

The system equations can be rewritten to separate voltage drops of the stationary fundamental component from voltage drops caused by transients and spatial harmonics as given on the right-hand side of (4) and (5). Herein  $\bar{i}_k$  denotes the fundamental component of the stationary current and  $\bar{\Psi}_k$  of the flux linkage. The stationary fundamental component flux linkages only depend on the currents and not on the rotor angle. Consequently, only two-dimensional flux linkage functions as shown in Fig. 3 (b) are needed in the following. The expression  $\Delta v_{k,machine}$  sums up effects of flux linkage changes due to current and angular changes. These are interpreted as voltage errors of the machine because they subsume voltage differences of the real machine to the stationary fundamental component machine model.

The machine stator voltage  $v_k$  is supplied by an inverter which is a nonlinear voltage source. The inverter output voltage  $v_k$  differs from the reference voltage  $v_k^*$  which is called voltage error and denoted  $\Delta v_{k,inverter}$  in the following. Voltage errors are of numerous origins [1, 2, 4, 5]: forward voltage and differential resistance of diodes and switches, switching time and switching behavior, dead-times, minimal on- and off-times and current zero-clamping. A simple inverter model including all these effects is a time-dependent voltage source  $v_k$  in the rotor-oriented dq-reference frame. As given on the left-hand side of (4) and (5) the inverter output voltage  $v_k$  can be split in the controller reference voltage  $v_k^*$  and the respective voltage error  $\Delta v_{k,inverter}$  with all quantities being time-dependent.

$$\underbrace{v_d^* + \Delta v_{d,inverter}}_{v_d} = R \cdot \bar{i}_d - \omega \bar{\Psi}_q(\bar{i}_d, \bar{i}_q) + \Delta v_{d,machine} \quad (4)$$

$$\underbrace{v_q^* + \Delta v_{q,inverter}}_{v_q} = R \cdot \bar{i}_q + \omega \bar{\Psi}_d(\bar{i}_d, \bar{i}_q) + \Delta v_{q,machine} \quad (5)$$

If the voltage errors  $\Delta v_{k,inverter}$  and  $\Delta v_{k,machine}$  are ignored in the current controller design, the machine currents will not be constant during stationary operation. This is true since the voltage errors cause the currents to change from one control period to another as depicted in Fig. 2 (b) by the red arrow. The current controller reacts to the current control deviation resulting in oscillatory behavior and increased current harmonics. In order to avoid that problem, the voltage errors have to be compensated. This is a challenging task because the voltage errors depend on almost all inverter and machine state variables and parameters. They change with the currents  $i_d$  and  $i_q$ , the rotor angle  $\gamma$ , the rotor speed  $n$ , the DC link voltage and the diode and switch parameters that depend both on temperature and age. If the voltage errors are identified online during drive operation these state and parameter dependencies are not a problem because any voltage error change is continuously identified and tracked. Thus, a method has to be developed that allows the online identification of the voltage errors. Then a proper compensation scheme can be designed which is described next.

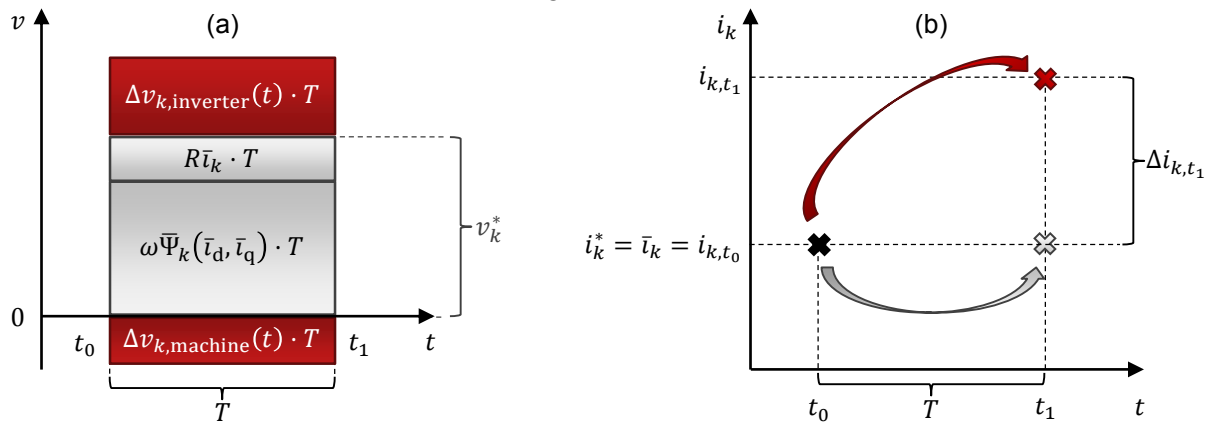


Fig. 2 Voltage components (a) and current samples (b) are given for one control period. Due to voltage errors a current control deviation  $\Delta i_{k,t_1}$  occurs which can be used to estimate the total voltage error.

## 2.2. Identification and Mitigation Method

In Fig. 2 (a) the voltage components of (4) and (5) are shown for quasi-stationary operation for one control period. The respective measured current samples  $i_{k,t_0}$  at the beginning and  $i_{k,t_1}$  at the end of the control period are drawn in Fig. 2 (b). In this example the current  $i_{k,t_0}$  is identical with the reference value  $i_k^*$ . If the voltage  $v_k^*$  is applied,  $i_{k,t_1}$  will also coincide with the reference value. However, a current control deviation  $\Delta i_{k,t_1}$  occurs due to the voltage errors. This deviation can be used to estimate the total voltage error by a calculation. A proportional element  $k_P$  can be used for that purpose. The voltage error is repeatedly adjusted by  $\Delta(\Delta\hat{v}_k) = k_P \cdot \Delta i_k$  and stored in dependence on the rotor angle  $\gamma$  as depicted in the memory block of Fig. 1. The memory block is periodically updated and the stored voltage errors  $\Delta\hat{v}_{k,\gamma}$  are used for feed-forward control when the rotor returns to the same position. The algorithm converges within a few electric periods because all processes are periodical during quasi-stationary operation. The machine currents  $i_d$  and  $i_q$ , the rotor speed  $n$ , the DC link voltage and the diode and switch parameters do not change or only change with a slow rate. Hence, the memory block is the rotor angle dependent integral term of the current controller and the method works without an inverter and machine model.

A better voltage error estimation and faster convergence is obtained by using a fundamental component machine model. It is important to notice that the machine model is not obligatory but only used for faster convergence. The ohmic stator resistance and the stationary flux linkage functions of the fundamental component are obtained by offline measurements [12] and needed as model parameters. Parameter errors are interpreted as voltage errors and therefore automatically compensated. The voltage  $\hat{v}_{k,\text{machine}}$  that causes the current to change from  $i_{k,t_0}$  to  $i_{k,t_1}$  is calculated using the machine's system equations.

$$\hat{v}_{d,\text{machine}} = \frac{1}{2}R(i_{d,t_0} + i_{d,t_1}) + \frac{\Psi_{d,t_0} - \Psi_{d,t_1}}{T} - \frac{1}{2}\omega(\Psi_{q,t_0} + \Psi_{q,t_1}) \quad (6)$$

$$\hat{v}_{q,\text{machine}} = \frac{1}{2}R(i_{q,t_0} + i_{q,t_1}) + \frac{\Psi_{q,t_0} - \Psi_{q,t_1}}{T} + \frac{1}{2}\omega(\Psi_{d,t_0} + \Psi_{d,t_1}) \quad (7)$$

Thereby  $T$  denotes the control period duration and  $\Psi_{k,t_0}$  and  $\Psi_{k,t_1}$  the flux linkages that can be calculated from  $i_{k,t_0}$  and  $i_{k,t_1}$  by the flux linkage functions shown in Fig. 3 (b). Equations (6) and (7) are a time-discrete solution of (1) and (2) with the approximations that the dynamic ohmic voltage drop is negligible and that the flux linkages change linearly. The precise deduction and the validity of the approximations for the machine under test are given in [12]. With  $v_k^*$  as controller reference voltage the total voltage error  $\Delta\hat{v}_k$  is obtained and stored in the memory block as described above.

$$\Delta\hat{v}_d = \Delta v_{d,\text{inverter}} + \Delta v_{d,\text{machine}} = v_d^* - \hat{v}_{d,\text{machine}} \quad (8)$$

$$\Delta\hat{v}_q = \Delta v_{q,\text{inverter}} + \Delta v_{q,\text{machine}} = v_q^* - \hat{v}_{q,\text{machine}} \quad (9)$$

As shown in Fig. 1 the identification and memory block are inserted in parallel to a conventional current control structure. The current controller described in [12] is used to calculate the inverter reference voltages  $v_k^*$ . After back-transformation to stator voltages, a modulator creates the gate signals for the inverter. The stator currents and the rotor angle are measured to realize closed-loop rotor-oriented current control.

## 3. Experimental Setup

Experiments are conducted with a permanent-magnet reluctance torque synchronous machine of type *Brusa HSM1-6.1712-CO1*. The machine's properties are given in Fig. 3 (a) and its nonlinear flux linkage functions obtained by stationary measurements in Fig. 3 (b) [12]. The flux linkages depend nonlinearly on both currents due to saturation and cross-coupling.

Inverters for grid connection and control of both machines switching at 8 kHz are based on *Semikron SkiiP 513GD122-3DUL* modules. In order to operate the machine with nominal voltage a DC link voltage of 300 V and space vector modulation is used. Currents are measured by the built-in *Semikron SkiiP* current transducers. Speed and rotor angle are calculated using the machine's built-in incremental encoder signals. For central data capturing

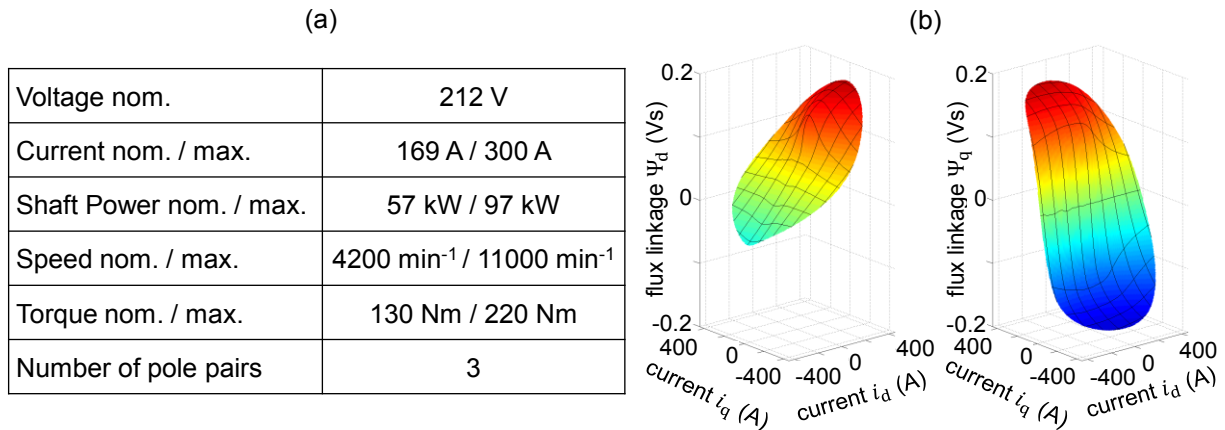


Fig. 3 The machine properties are given in (a). The motor under test has highly nonlinear magnetics as can be seen in the measured flux linkage functions  $\Psi_d = f(i_d, i_q)$  and  $\Psi_q = g(i_d, i_q)$  (b).

a digital signal processor system is used to record phase currents, speed and rotor angle data with a sampling rate of 8 kHz.

The proposed method is implemented on the digital signal processor (DSP) *TMS320C6748* produced by *Texas Instruments*. One hundred rotor angle supporting points are used to store the voltage errors  $\Delta\hat{v}_k$  resulting in a total memory demand of 800 byte at single precision. Additional calculation time is almost negligible because only a few additions, subtractions and multiplications of (6) to (9) are performed. To realize a switching frequency of 8 kHz all calculations are executed within less than 125  $\mu$ s. Inverter gate signals are created by a modulator using a field programmable gate array (FPGA) of the *Cyclone* series by *Altera*.

## 4. Results and Discussion

In order to evaluate the experimental performance of the described method three different controller setups and mitigation techniques are compared:

- First, a PI-type controller with no compensation (plots (a) in Fig. 4 and Fig. 6).
- Second, an advanced PI-type controller [13] with compensation of the dead-time in the modulator. This is a conventional compensation method and similar to the method described in [1] (plots (b) in Fig. 4 and Fig. 6).
- Third, the proposed method as shown in Fig. 1 and described in Section two (plots (c) in Fig. 4 and Fig. 6).

The mitigation performance is analyzed by means of nominal operation, by a continuous power profile and in the total operational area.

### 4.1. Nominal Operation

The point of nominal operation at a rotor speed of 4200 min<sup>-1</sup> and a torque of 130 Nm is marked by dark grey crosses in all plots of Fig. 6. The corresponding measured currents are shown for the three methods in the graphs of Fig. 4. Results of the proposed method are given in (c). The current ripples are significantly lower in comparison to the PI-type controller with compensation (b) and without compensation (a). In both (a) and (b) the current oscillates in a repetitive manner which is caused by the voltage errors of the machine and the inverter. In contrast, the proposed method (c) mitigates all harmonics. Due to the functional principle of the method any systematic oscillation of the current is removed which is why the current only contains noisy jittering besides the fundamental component. This is realized by feed-forward control of the online identified voltage errors shown in the memory block of Fig. 1. In order to compare the performance of the three methods the total harmonic distortion (THD) is calculated using the measured current samples.

$$\text{THD}_{4\text{kHz}} = \frac{\sqrt{I^2 - I_1^2}}{I_1} \quad (10)$$

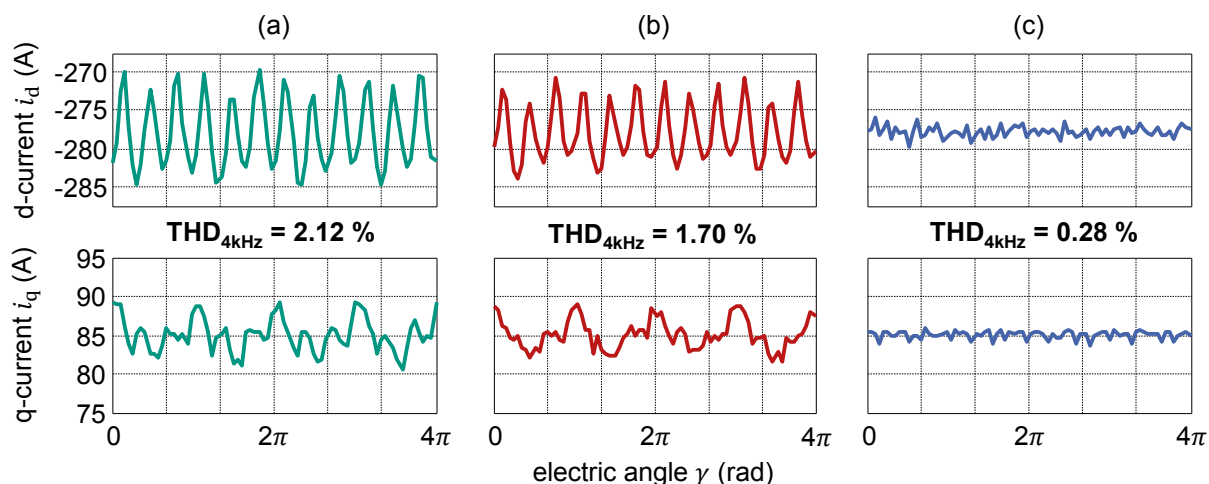


Fig. 4 Measured currents at nominal operation with  $\bar{i}_d = -277.9$  A and  $\bar{i}_q = 85.0$  A. Results of the PI without compensation (a), of the PI with compensation (b) and of the proposed method (c) are shown. The THD of the proposed method is significantly lower in comparison to the conventional methods.

Therein  $I$  denotes the effective phase current for frequencies up to 4 kHz and  $I_1$  the effective phase current of the fundamental component. The proposed method (c) significantly reduces the THD to 0.28 % which is less than a seventh of the value without compensation (a).

The absolute value of each harmonic  $|i_{FFT}|$  of the measured dq-currents of Fig. 4 is calculated by Fourier transformation and given in Fig. 5 (a). The spectra of the conventional compensation and the no compensation method dominantly contain harmonics of the sextuple of the fundamental frequency. This is true because for example the  $-5^{\text{th}}$  and  $7^{\text{th}}$  phase current harmonics are transformed to a  $6^{\text{th}}$  in the dq-reference frame. Moreover, a  $2^{\text{nd}}$  and  $4^{\text{th}}$  harmonic is visible in the current spectra. These are caused by the not perfectly symmetrical winding of the machine under test. The  $2^{\text{nd}}$  current harmonic is mostly the dq-transformed negative sequence component of the fundamental. A  $\pm 3^{\text{rd}}$  voltage harmonic is in-phase in the three machine phases and caused by modulation zero-sequence voltage components and saturation harmonics. Due to winding asymmetry these do not cancel each other out, which is why the  $2^{\text{nd}}$  and  $4^{\text{th}}$  dq-transformed current harmonics are obtained. The proposed method however, reduces all harmonics regardless of their physical origin or frequency. Current harmonic mitigation is only limited by the sampling frequency and the inverter voltage limit.

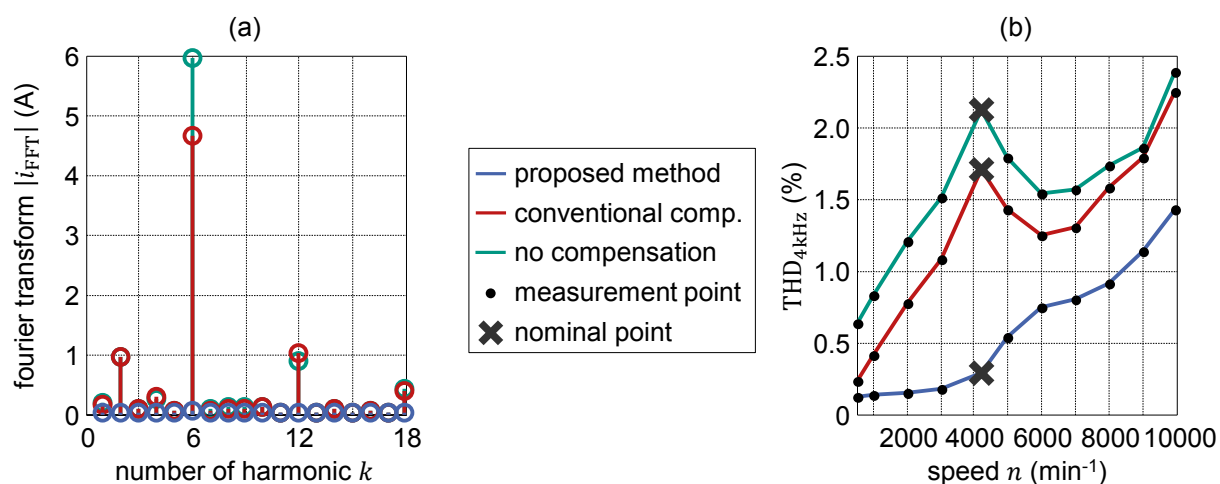


Fig. 5 The Fourier transforms of the measured currents of Fig. 4 are given in (a). The THD calculated by (10) for the continuous power profile marked in light grey in Fig. 6 is shown in (b). The mitigation performance is remarkably lower in both plots using the proposed method.

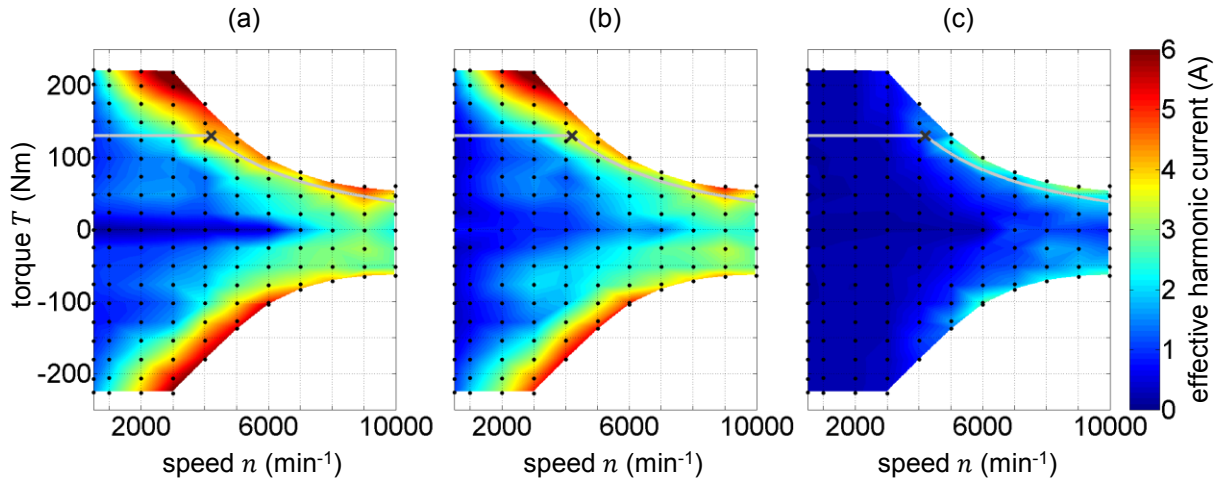


Fig. 6 The three methods are analyzed in the total operational area of the machine. The effective harmonic current is the lowest for the proposed method (c) in comparison to the PI controller with compensation (b) and the PI controller without compensation (a).

## 4.2. Continuous Power Profile

A load profile of continuous power is marked by the light grey line in all graphs of Fig. 6. Starting from standstill the torque is kept constant until the nominal operation point is reached. Afterwards the mechanical power is linearly reduced to 70 % of the nominal power at maximum speed. The THD is calculated for the continuous power profile for the three methods and shown in Fig. 5 (b). The THD of the conventional and no compensation method increase at first because harmonics increase due to the higher stator frequency. In the field weakening regime the THD is reduced up to a speed of 6000  $\text{min}^{-1}$  because the differential inductances increase which prevails the effect of the rising stator frequency. The THD of the proposed method is lower along the whole load profile curve. It increases in the field weakening regime because the inverter can neither supply the needed frequency nor the voltage to completely mitigate the current harmonics.

## 4.3. Total Operational Area

The effectiveness of the three methods is analyzed in the whole operational area by comparison of the effective harmonic current as shown in Fig. 6 (a) to (c). There, measurement points are marked by black dots and bilinear interpolation is used to calculate data in between. Reference values of minimal stator current amplitude with respect to the voltage constraint are used [14]. Current harmonics of the proposed method (c) are lower in the total operational area in comparison to the method with conventional compensation (b) and with no compensation (a). The current harmonics are increased towards the maximum torque in (a) and (b) because of lower differential inductances due to iron saturation. Moreover, the influences of the inverter voltage limit are visible, because the effective harmonic current is increased in the field weakening regime when the inverter cannot supply the needed voltage and frequency for mitigation.

## 5. Conclusion

A control method is described that mitigates all current harmonics independent on their physical origin. Mitigation capability is only limited by the sampling frequency and the inverter voltage limit. The method is based on online identification, rotor angle dependent storage and precise feed-forward control of the voltage errors. It basically works without an inverter and machine model, but convergence is improved if a fundamental component machine model is used for voltage error identification. The effectiveness of the proposed method is proven by

measurements which show that the current harmonics are significantly reduced under all operational conditions of the machine under test. Implementation of the method in existing inverters is easy. It can be realized by software updates because only the already available current and rotor angle sensors are needed. The method is micro-controller capable and extra need of calculation time and dynamic memory is very little. The used functional principle is transferable to other machine types and grid applications enabling the mitigation of current harmonics in a wide field of applications.

## 6. References

- [1] T. Sukagawa, K. Kamiyama, K. Mizuno, T. Matsui, and T. Okuyama, "Fully digital, vector-controlled PWM VSI-fed ac drives with an inverter dead-time compensation strategy," *IEEE Trans. Industry Applications*, vol. 27, no. 3, pp. 552-559, May/June 1991.
- [2] J.-W. Choi, and S.-K. Sul, "A new compensation strategy reducing voltage/current distortion in PWM VSI systems operating with low output voltages," *IEEE Trans. Industry Applications*, vol. 31, no. 5, Sep./Oct. 1995.
- [3] A.R. Munoz, and T.A. Lipo, "On-line dead-time compensation technique for open-loop PWM-VSI drives," *IEEE Trans. Power Electronics*, vol. 14, no. 4, pp. 683-689, July 1999.
- [4] H.-S. Kim, K.H. Kim, and M.-J. Youn, "On-line dead-time compensation method based on time delay control," *IEEE Trans. Control Systems Technology*, vol. 11, no. 2, pp. 279-285, March 2003.
- [5] N. Urasaki, T. Senjyu, T. Kinjo, T. Funabashi, and H. Sekine, "Dead-time compensation strategy for permanent magnet synchronous motor drive taking zero-current clamp and parasitic capacitance effects into account," *IEE Proc. Electric Power Applications*, vol. 152, no. 4, pp. 845-853, July 2005.
- [6] S. L. Kellner, K. Beer, and B. Piepenbreier, "Compensation of PWM inverter voltage errors based on measurement of DC-link and output voltages," *Conference Record of the PCIM Europe*, Nuremberg, Germany, 2011.
- [7] R. Michel, "Kompensation von sättigungsbedingten Harmonischen in den Strömen feldorientierter Synchronmotoren," dissertation TU Dresden, Vieweg+Teubner, Wiesbaden, 2009.
- [8] F. Mink, "Modellierung und hochdynamische Stromregelung von PM-Synchronmaschinen unter Berücksichtigung von Sättigungseffekten," dissertation TU Darmstadt, Ingenieurwissenschaftlicher Verlag, Bonn, 2013.
- [9] M. Tomizuka, T.-C. Tsao, and K.-K. Chew, "Analysis and synthesis of discrete-time repetitive controllers," *Journal of Dynamic Systems, Measurement and Control*, vol. 111, issue 3, pp. 353-358, Sept. 1989.
- [10] J.-H. Moon, M.-N. Lee, and M. J. Chung, "Repetitive control for the track-following servo system of an optical disk drive," *IEEE Trans. Control Systems Technology*, vol. 6, no. 5 Sep. 1998.
- [11] J. Richter, P. Winzer, and M. Doppelbauer, "Einsatz virtueller Prototypen bei der akausalen Modellierung und Simulation von permanenterregten Synchronmaschinen", *ETG Fachbericht Band 139*, VDE Verlag GmbH Berlin Offenbach, 2013.
- [12] J. Richter, T. Gemaßmer, and M. Doppelbauer, "Predictive current control of saturated cross-coupled permanent magnet synchronous machines", *Conference Record of the Symposium on Power Electronics, Electrical Drives, Automation and Motion*, p. 830-835, Ischia, Italy, 2014.
- [13] T. Gemaßmer, J. Richter, M. Schnarrenberger, and M. Braun, "High dynamic rotor oriented control for permanent magnet synchronous machines with saturation characteristics," *Conference record of the PCIM Europe*, Nuremberg, Germany, 2014
- [14] S. Morimoto, M. Sanada, and Y. Takeda, "Wide-speed operation of interior permanent magnet synchronous motors with high performance current regulator," *IEEE Trans. Industry Applications*, vol. 30, issue 4, pp. 920-926, Jul.-Aug. 1994.